



**Romanian Academy
„Ilie Murgulescu” Institute of Physical Chemistry**

THESIS SUMMARY

Thermodynamic properties of nanostructured oxide materials for sensors applications

Scientific advisor:

CS I Dr. Tănăsescu Speranța Valeria

**PhD student,
Ciobota (Ruști) Cristina Florentina**

BUCHAREST 2017

SUMMARY

Part I State of the Art	1
Chapter 1. INTRODUCTION	2
Chapter 2. STATE OF THE ART REGARDING OXIDE PEROVSKITE NANOMATERIALS WITH POTENTIAL APPLICATION IN GAS SENSORS	
2.1 General considerations regarding gas sensors	8
2.1.1 Obtaining methods for metal oxide based gas sensors	10
2.1.2 Gas Detection Mechanism	11
2.1.3 Oxide materials used in gas sensors	14
2.2 Perovskite compounds used in gas sensor	24
2.2.1 General considerations regarding perovskite structure	24
2.2.2 Goldschmidt tolerance factor and structural parameters in compounds with perovskite structure.	26
2.2.3 Barium titanate (BaTiO ₃) structure	28
2.2.4 Defect chemistry in BaTiO ₃ . Correlations between defect chemistry and electrical conductivity	31
2.3 Thermodynamic study of nanocrystalline materials with potential application in gas sensors	43
2.3.1 Particularities of phase transformations in nanocrystalline systems	43
2.3.2 Thermal stability of nanocrystalline materials. Particularities of the grain growth process	45
2.3.3 Conclusions on the thermodynamic behavior of nanocrystalline perovskites.	52
The need for additional contributions in the field of study.	
Part II EXPERIMENTAL PART	55
Chapter 3. EXPERIMENTAL METHODS FOR CHARACTERIZATION	56
3.1 Brunauer-Emmett-Teller (BET) Specific Surface Measurements	56
3.2 Particle size distribution by Dynamic Light Scattering measurement (DLS)	58
3.3 Experimental techniques of structural and morphological analysis	59
3.4 Thermal analysis and calorimetry techniques	62
3.5 Thermomechanical analysis (TMA)	67
3.6 EFM measurements associated with solid state coulometric titration technique	69
3.7 Impedance spectroscopy measurements	73
PART III : ORIGINAL CONTRUBUTIONS	74
Chapter 4. MATERIAL SYNTHESIS	75
4.1 Thermodynamic prediction of hydrothermal reaction	75
4.2 Stages of materials hydrothermal synthesis	78
4.3 Hydrothermal synthesis of strontium doped barium titanate (BST) and strontium and copper doped barium titanate (BST_Cu)	80
4.4 Chemical analysis of hydrothermally obtained powders	82
4.5 Partial conclusions. Original contributions	83
Chapter 5 STUDY OF NANOSTRUCTURED Ba_{0.75}Sr_{0.25}TiO₃ (BST) POWDER OBTAINED BY HYDROTHERMAL SYNTHESIS	84
5.1 Brunauer-Emmett-Teller (BET) Specific Surface Measurements	
5.2 Particle size distribution by Dynamic Light Scattering measurement (DLS)	85
5.3 Experimental techniques of structural and morphological analysis	86
5.4 Study of the thermodynamic stability of Ba _{0.75} Sr _{0.25} TiO ₃ nanostructured powders synthesized by hydrothermal process	90
5.5 Structural and morphological analysis of thermally treated samples at 1073K	98
5.6 Electromotive force measurements (EFM)	104
5.7 Oxygen stoichiometry variation influence on thermodynamic properties. EFM measurements coupled with solid coulometric titration	107
5.8 Partial conclusions. Original contributions	109
Capitolul 6 STUDY OF NANOSTRUCTURED (Ba_{0.75}Sr_{0.25}) (Ti_{0.95}Cu_{0.05})O₃ (BST_Cu) POWDER OBTAINED BY HYDROTHERMAL SYNTHESIS	110

6.1 Brunauer-Emmett-Teller (BET) Specific Surface Measurements	110
6.2 Particle size distribution by Dynamic Light Scattering measurement (DLS)	113
6.3 Structural and morphological characterization of perovskite powders	115
6.4 Study of thermodynamic stability of nanostructured powders $(\text{Ba}_{0.75}\text{Sr}_{0.25})(\text{Ti}_{0.95}\text{Cu}_{0.05})\text{O}_3$ synthesized by hydrothermal process	120
6.5 Thermomechanical analysis (TMA)	126
6.6 Structural and morphological analysis of thermal treated BST_Cu at 1123 K (BST_Cu1123)	128
6.7 Electromotive force measurements (EFM)	131
6.8 Oxygen stoichiometry variation influence on thermodynamic properties	134
6.9. Partial conclusions. Original contributions	136
Chapter 7 ELECTRICAL PROPERTIES (RESISTANCE, RESISTIVITY, CONDUCTIVITY) DETERMINATION USING IMPEDANCE SPECTROSCOPY MEASUREMENTS	137
7.1 Resistance, resistivity and conductivity determination of nanostructured BST and BST_Cu samples using impedance spectroscopy measurements	137
7.2 Correlations between thermodynamic properties, electrical conductivity and thermal expansion in 823-1273 K temperature range.	140
Chapter 8 OBTAINING AND EVALUATION OF $\text{Ba}_{0.75}\text{Sr}_{0.25}\text{TiO}_3$ and $(\text{Ba}_{0.75}\text{Sr}_{0.25})(\text{Ti}_{0.95}\text{Cu}_{0.05})\text{O}_3$ OXIDES BASED GAS SENSOR PERFORMANCE	143
8.1 Partial conclusions. Original contributions	148
Chapter 9 FINAL CONCLUSIONS. ORIGINAL CONTRIBUTIONS	149
BIBLIOGRAPHY	153
List of published papers related to the thesis topic	177
PATENTS	178
List of communications presented at national and international scientific events	178

KEYWORDS: nanostructured materials, hydrothermal synthesis, thermodynamics properties, electrical properties, gas sensors, doped barium titanate

INTRODUCTION

Among the compounds with perovskite structure, barium titanate (BaTiO_3), as well as solid solutions obtained by the substitution of Ba^{2+} and Ti^{4+} ions with other elements, are highly studied materials due to their applications in the electronic components. There are also a number of studies regarding the use of these materials in different types of sensors. Thus, $\text{Ba}_{1-x}\text{Sr}_x\text{TiO}_3$ is a particularly attractive material for IR sensors, wireless temperature sensors, humidity and gas sensors.

Sensitivity to analyte gas, selectivity and durability are the most important properties of a gas sensor. The detection mechanism is based on the resistivity change after the sensor has been exposed to the analyzed gas. Perovskite oxides microstructure modification by using different synthetic methods, as well as modification of various compositional variables such as the nature and concentration of donor or acceptor type dopants are essential for obtaining optimum electrical and transport characteristics. In addition, heat treatment is an important step not only to ensure stability, but also to control structural defects and grain size, also contributing to sensitivity and selectivity of the sensors.

Despite the interest and the research effort in this field, many aspects of finding appropriate processing parameters and, above all, the fundamental understanding of the correlations between all the factors that ensure the optimization of the sensor's functioning are not yet elucidated.

In order to bring original contributions to the proposed topic, a systematic thermodynamic study of the thermodynamic stability domains and of the correlations between the composition, structure, electrical and thermodynamic properties of some barium titanate-based nanostructured materials with potential use in gas sensors applications has been done. For this study, two compositions obtained by the A- and B-site barium titanate substitution, namely $\text{Ba}_{0.75}\text{Sr}_{0.25}\text{TiO}_3$ and $(\text{Ba}_{0.75}\text{Sr}_{0.25})(\text{Ti}_{0.95}\text{Cu}_{0.05})\text{O}_3$ were selected. The research is based on a complex thermodynamic approach, taking into account the following aspects: identification of energetic parameters that favor the stability of nanostructured phases; the correlation of the thermodynamic quantities with structure, composition, thermal expansion and electrical properties in wide temperature ranges; the study of the correlative effects of temperature and structural defects on the thermodynamic behavior of the samples; the influence of various compositional variables (composition, microstructure, oxygen non-stoichiometry) on energetic parameters and sensors performances of the studied materials.

Taking into account the approached field, the thesis pursued the following **specific objectives**:

1. Synthesis of $\text{Ba}_{0.75}\text{Sr}_{0.25}\text{TiO}_3$ si $\text{Ba}_{0.75}\text{Sr}_{0.25}\text{Ti}_{0.95}\text{Cu}_{0.05}\text{O}_3$ nanostructured powders using hydrothermal method. Given the importance of judicious choice of reagents used in the process of obtaining nanostructured powders, the selection of raw materials was based on the thermodynamic prediction (using the HSC 8 Outotec software) taking into account the physico-chemical properties of the inorganic precursor salts.

2. Structural, morphological and surface characterization of powders obtained by the hydrothermal method. Structural and morphological characterization of samples was performed by X-ray diffraction (XRD), scanning electron microscopy (SEM, EDS), electron spin resonance (ESR) and Raman spectroscopy. The specific surface area and the porosity of the samples were determined by the Brunauer-Emmett-Teller (BET) method. In order to identify the intermediate phases formed in the process of heating of the nanostructured powders and, at the same time, to evaluate the relationship between the structure evolution and the changes with temperature of thermodynamic parameters, the structural and morphological analysis on the powders resulting after the thermal treatment at 1073 K followed by cooling at room temperature has been performed.

3. Thermodynamic and thermochemical study of $\text{Ba}_{0.75}\text{Sr}_{0.25}\text{TiO}_3$ and $(\text{Ba}_{0.75}\text{Sr}_{0.25})(\text{Ti}_{0.95}\text{Cu}_{0.05})\text{O}_3$ nanocrystalline powders synthesized by the hydrothermal process. The thermodynamic functions under isothermal conditions (relative enthalpy, heat capacity, relative entropy and Gibbs free energy) of the compounds investigated by drop calorimetry method have been determined for the first time within this thesis. Thermochemical behavior under heating conditions was analyzed using methods specific to thermal analysis, namely dynamic differential scanning calorimetry (DSC) coupled with

thermogravimetry (TG). In addition, the correlative effect of temperature and defect structure on the thermodynamic behavior of the samples was discussed based on the evolution of the thermodynamic quantities of the oxygen dissolution in the perovskite structure, which were also obtained for the first time in this thesis by using electromotive force measurements on solid electrolyte electrochemical cells (EMF) under equilibrium conditions. Oxygen stoichiometry variation effect on thermodynamic properties was evidenced by coupling the EMF measurements with solid state coulometric titration. *The study allowed discussion of the composition-microstructure-thermodynamic properties correlations and underlined the role of the energetic parameters in controlling the stability of materials at nanoscale.*

4. Thermal expansion study in temperature range of 350-1273 K and highlighting correlations between thermodynamic stability, microstructure and thermal expansion.

5. Electrical properties of $Ba_{0.75}Sr_{0.25}TiO_3$ and $(Ba_{0.75}Sr_{0.25})(Ti_{0.95}Cu_{0.05})O_3$ nanocrystalline powders synthesized by the hydrothermal process. The resistance, resistivity and electrical conductivity of materials synthesized by the hydrothermal method were determined and the change of electrical properties with temperature and composition has been investigated. *The study allowed highlighting the correlations between the electrical properties, the thermodynamic quantities and the structural characteristics of the investigated compounds.*

6. Evaluation of the sensorial properties of $Ba_{0.75}Sr_{0.25}TiO_3$ and $(Ba_{0.75}Sr_{0.25})(Ti_{0.95}Cu_{0.05})O_3$ oxide materials. The sensory performances (sensitivity, selectivity, stability, response time and recovery time) of the exposed oxides to H_2S in different humidity environments were investigated and discussed.

Thesis structure:

The PhD thesis is structured in 9 chapters, divided into 3 distinct parts:

Part I: The Current State of the Art (Chapters 1 and 2)

Part II: Experimental characterization methods (Chapter 3)

Part III: Original contributions (Chapters 4, 5, 6, 7, 8 and 9)

The thesis ends with bibliographic references.

In **Chapter 1, Introduction**, after a brief presentation of the importance of the field addressed, the aim, the specific objectives and the structure of the thesis are highlighted.

Chapter 2 contains a description of the current level of research in the field of oxide materials potentially used in gas sensors, insisting on perovskite structured materials. Based on bibliographic research, the main theoretical and experimental aspects regarding the role of the energetic parameters in the understanding and the control of the nanostructured material's stability are critically discussed. At the same time the need for contributions in the domain is identified.

Chapter 3 contains the presentation of the experimental methods and techniques used for the physicochemical characterization (BET, XRD, SEM, RES, RAMAN, DSC/TG, drop calorimetry, FEM, solid state coulometric titration, TMA, impedance spectroscopy), insisting on thermodynamic and thermochemical characterization methods.

Chapter 4 contains original contributions regarding the hydrothermal synthesis of $Ba_{0.75}Sr_{0.25}TiO_3$ and $(Ba_{0.75}Sr_{0.25})(Ti_{0.95}Cu_{0.05})O_3$ materials. The considerations underlying the selection of the starting materials are presented and the technological flow and the synthesis conditions for obtaining $Ba_{0.75}Sr_{0.25}TiO_3$ and $(Ba_{0.75}Sr_{0.25})(Ti_{0.95}Cu_{0.05})O_3$ nanostructured powders are described according to Application of patent no. OSIM A 00794 / 27.10.2014.

Chapter 5 contains original contributions regarding experimental results obtained from the study carried out on the $Ba_{0.75}Sr_{0.25}TiO_3$ nanostructured powders. The powders were structurally and morphologically characterized, the specific surface and porosity were determined, the thermodynamic functions and the thermochemical stability of the micro- and nanostructured powders were determined and thermal expansion were determined.

Chapter 6 contains original contributions obtained from the study of nanostructured powders with the composition $(Ba_{0.75}Sr_{0.25})(Ti_{0.95}Cu_{0.05})O_3$. The microstructure, morphology and surface

characteristics, the thermodynamic and thermochemical properties, as well as thermal expansion of the micro and nanostructured phases were analyzed.

Chapter 7 contains the original contributions regarding the measurements of electrical properties (resistance, resistivity and conductivity) obtained by impedance spectroscopy method and evaluation of the correlations between the electrical properties and the thermodynamic properties of $\text{Ba}_{0.75}\text{Sr}_{0.25}\text{TiO}_3$ and $(\text{Ba}_{0.75}\text{Sr}_{0.25})(\text{Ti}_{0.95}\text{Cu}_{0.05})\text{O}_3$ powders synthesized by hydrothermal method.

Chapter 8 contains original contributions referring to the assessment of the sensorial properties of $\text{Ba}_{0.75}\text{Sr}_{0.25}\text{TiO}_3$ and $(\text{Ba}_{0.75}\text{Sr}_{0.25})(\text{Ti}_{0.95}\text{Cu}_{0.05})\text{O}_3$ oxide films.

Chapter 9 contains the final conclusions of the present study.

Materials synthesis

Pourbaix diagrams provided data based on which the studied compounds were obtained. Hydrothermal synthesis allowed the nanostructured crystalline powders $\text{Ba}_{0.75}\text{Sr}_{0.25}\text{TiO}_3$ and $(\text{Ba}_{0.75}\text{Sr}_{0.25})(\text{Ti}_{0.95}\text{Cu}_{0.05})\text{O}_3$ to be obtained in a single step. For simplicity, the materials will be called BST and BST_Cu, respectively.

BET and DLS measurements. Structural and morphological characterization of nanostructured powders

The **surface area** and the **pores volume** of the sample BST_Cu are two times greater than the surface area and, respectively the pores volume of the BST sample. The mean **hydrodynamic diameter** of BST_Cu is much bigger (364 nm) than that of BST (51.4 nm). This is due to the agglomeration trend of BST_Cu particles that are smaller than those of BST. The **XRD analysis** of BST and BST_Cu samples at room temperature indicated the existence of the same phases in both BST and BST_Cu: tetragonal phase (PDF 70-9164), cubic phase (PDF 71-4894) as well as other secondary phases: the phase of whiterite (BaCO_3) and very small amounts of CuO . Instead, in the case of BST_Cu, the RES spectra (Figure 1) have highlighted broad peaks indicating the presence of dipolar interactions and the fact that Cu^{2+} ions are not evenly distributed. Spectrum asymmetry confirms the presence of Cu^{2+} in the distorted octahedral coordination state, even at 1123 K.

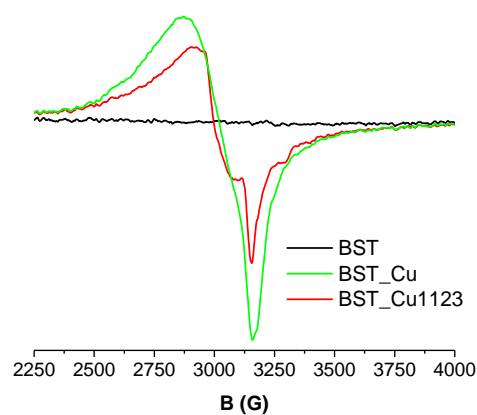


Figure 1. RES results of BST samples; BST_Cu and BST_Cu1123.

The SEM analysis (Fig. 2) revealed that the particle size of BST_Cu is smaller than the particle size of BST. The presence of copper in the strontium-doped barium titanate structure leads to distortion of the perovskite lattice, so that by changing the lattice parameters the particle size decreases.

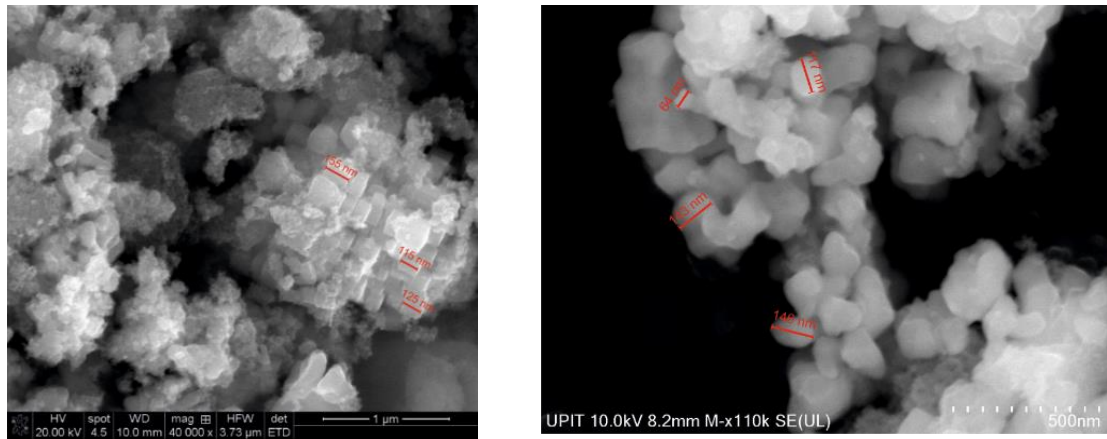


Figure 2. SEM analysis of BST powder (left) and BST_Cu (right).

The presence of Cu^{2+} at the Ti^{4+} positions will affect the Ti-O-Ti bond by forming new Cu-O-Ti or Cu-O-Cu bonds, as evidenced by the modification of the Raman active modes (Figure 3).

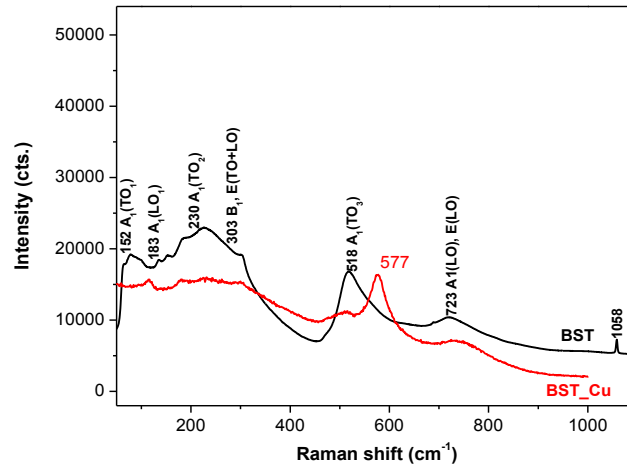


Figure 3. Raman spectra of BST and BST_Cu samples at room temperature in air.

Determination of thermodynamic functions: specific heat, relative entropy, Gibbs free energy function

For the first time, the thermodynamic functions in the isothermal conditions (relative enthalpy, heat capacity, relative entropy and Gibbs free energy) of $\text{Ba}_{0.75}\text{Sr}_{0.25}\text{TiO}_3$ and $(\text{Ba}_{0.75}\text{Sr}_{0.25})(\text{Ti}_{0.95}\text{Cu}_{0.05})\text{O}_3$ nanometer-sized powders synthesized by the hydrothermal method have been determined and energetic parameters favoring the stability of the nanostructured phases have been identified. The results obtained for the first time in this thesis for hydrothermal oxide powders confirm the increase of specific heat and entropy with the increase of nanocrystallinity (Fig. 4a), the minimum energy values indicating the range of stability of the nanostructured phases (Fig. 4b).

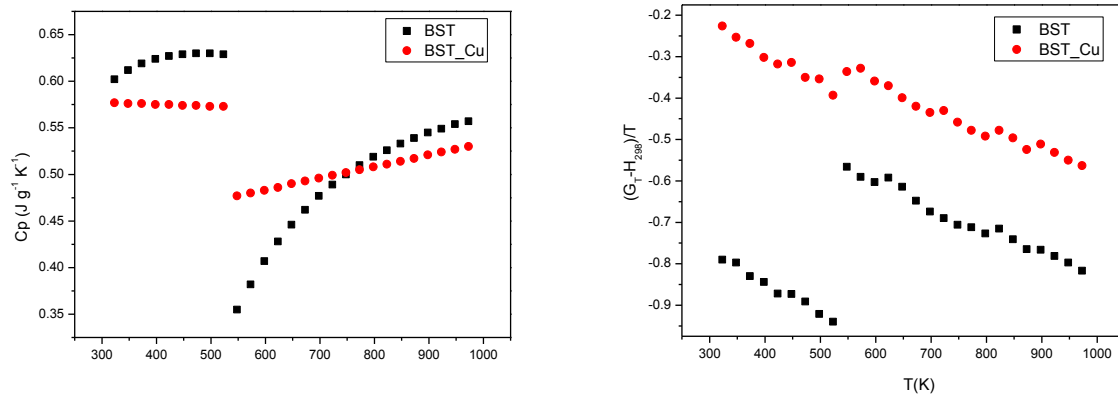


Figure 4. The temperature dependence of heat capacity (a) and Gibbs free energy function (b) for BST and BST_Cu samples

Electromotive force measurements (EMF)

The correlative effect of temperature and defect structure on the thermodynamic behavior of the BST and BST_Cu samples was discussed based on the evolution of the thermodynamic quantities of the oxygen dissolution in the perovskite phase, as measured by the EMF measurements. The thermodynamic quantities represented by the partial molar free energy ($\Delta\bar{G}_{O_2}$), enthalpy ($\Delta\bar{H}_{O_2}$) and entropy ($\Delta\bar{S}_{O_2}$) of the oxygen dissolution in the perovskite phase of BST and BST_Cu, as well as the equilibrium partial pressure of oxygen values were obtained for the first time in this thesis (Figure 5). Partial molar free energy is correlated with the concentration of oxygen vacancies; $\Delta\bar{H}_{O_2}$ can be considered as a measure of the binding strength of O^{2-} in oxide, and $\Delta\bar{S}_{O_2}$ as an indicator of O^{2-} ordering in the oxide. The obtained results reveal the increase of the thermodynamic instability with the increase of the temperature and the role of the charge compensation mechanism in explaining the structural changes of the analyzed samples. Both samples are thermodynamically more stable between 823-1073 K, at lower concentrations of oxygen vacancies.

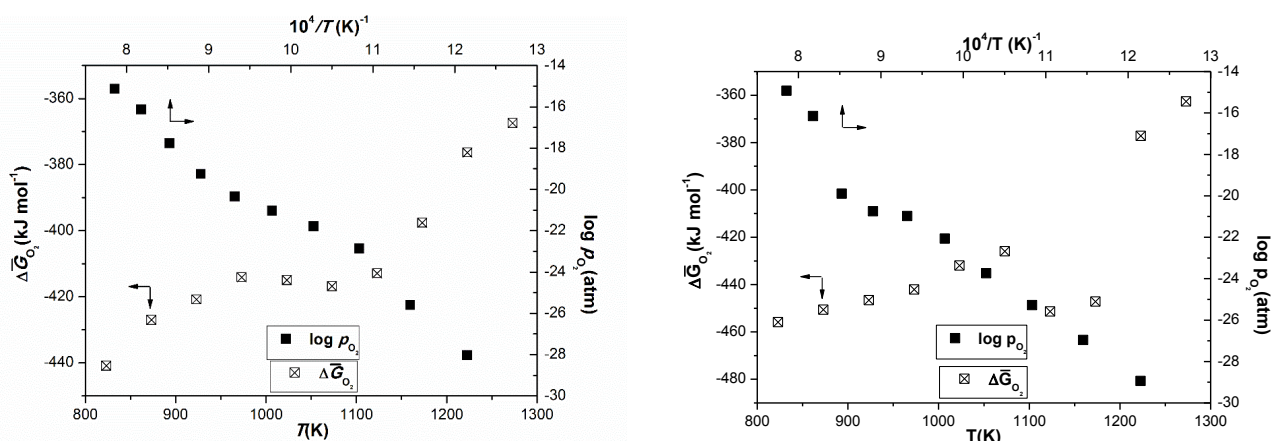


Figure 5. $\Delta\bar{G}_{O_2}$ and $\log p_{O_2}$ variation with temperature for BST (left) and BST_Cu (right)

EMF measurements coupled with solid state coulometric titration

Fig. 6 presents two sets of data experimentally obtained before and after isothermal titration. Changing oxygen stoichiometry ($-\Delta\delta = 0.02$) leads to decrease in $\Delta\bar{G}_{O_2}$ values that are an indicator for decreasing the concentration of oxygen vacancies. As the temperature rises, the $\Delta\bar{G}_{O_2}$ values move to higher values. The oxygen stoichiometry decreases as the temperature rises, which will lead to the formation of oxygen vacancies. The obtained results confirm that oxygen vacancies are generated at the expense of electron holes and confirms the strong effect of the charge compensation mechanism on the energetic parameters.

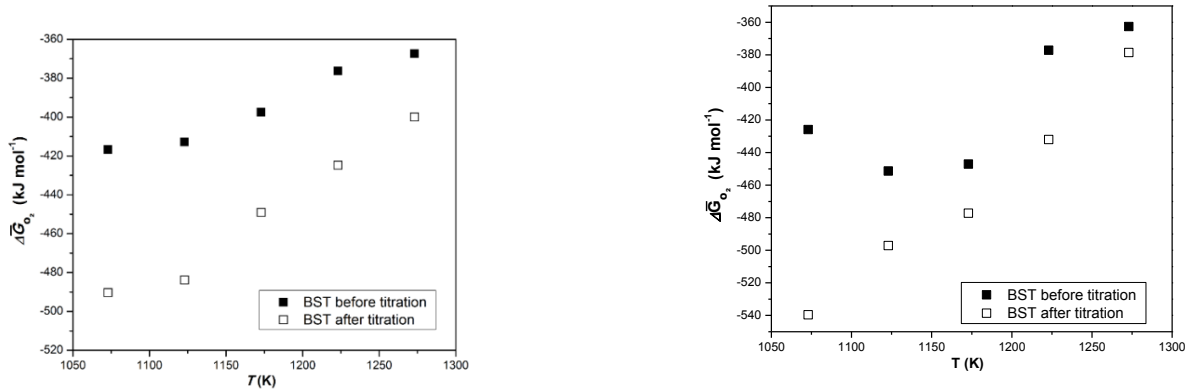


Figure 6. $\Delta\bar{G}_{O_2}$ variation with temperature and change of oxygen stoichiometry ($-\Delta\delta = 0.02$) for BST (left) and BST_Cu (right)

The variations $\Delta\bar{H}_{O_2}$ and $\Delta\bar{S}_{O_2}$ calculated in the range 1073-1273 K after titration are $-1373.54 \text{ kJ mol}^{-1}$ and $-774.61 \text{ J mol}^{-1}\text{K}^{-1}$, with approximately 273 kJ mol^{-1} and $223 \text{ J mol}^{-1}\text{K}^{-1}$ respectively lower than the enthalpy and entropy variations of the BST sample after titration. The strong decrease in enthalpy values suggests an increase in oxygen binding, and the decrease in entropy values indicates the increase in ordering of the oxygen sublattice of the perovskite structure.

Correlations between thermodynamic properties, electrical conductivity and thermal expansion in the temperature range 823-1273 K

Fig. 7 shows the variations in the conductivity of the BST and BST_Cu samples in the 823-1273 K temperature range; in the inset the evolution of the partial molar free energy of the samples in the same temperature range is presented. Conductivity activation energy values together the partial molar enthalpy and partial molar entropy values are shown in Table 1. Both the conductivity activation energy and the enthalpy and entropy variations of the BST_Cu sample are higher than the conductivity activation energy values, respective the thermodynamic quantities of the BST sample (Figure 7 and Table 1). Enthalpy values suggest that energetically favorable long range interactions between the charged defects that trap the oxygen vacancies become dominant in BST_Cu. In order to explain the conductivity discontinuity, it is also necessary to take into account the degree of ordering of the oxygen vacancies in the lattice together with the stress that develops in the material due to the oxygen concentration gradient, their contribution being supported by the results obtained by both the

variation of the thermodynamic quantities and that of thermal expansion (Figure 7). These results converge towards the idea of a strong link between thermodynamic, electrical properties and structural characteristics of the material.

Tabelul 1. Activation energy values, enthalpy variation $\Delta\bar{H}_{O_2}$ and entropy variation $\Delta\bar{S}_{O_2}$

Sample	Temperature range (K)	Activation energy (kJ mol ⁻¹)	$\Delta\bar{H}_{O_2}$ (kJ mol ⁻¹)	$\Delta\bar{S}_{O_2}$ (J mol ⁻¹ K ⁻¹)
BST	823-973	109.03	-581.18	-173.316
BST	1123 - 1273	176.57	-766.32	-315.340
BST_Cu	823-1023	121.57	-555.97	-120.06
BST_Cu	1073-1273	198.76	Due to the deviation from the linearity of the temperature variation of energy, in this temperature range $\Delta\bar{H}_{O_2}$ it is not calculated.	Due to the deviation from the linearity of the temperature variation of energy, in this temperature range $\Delta\bar{S}_{O_2}$ it is not calculated.

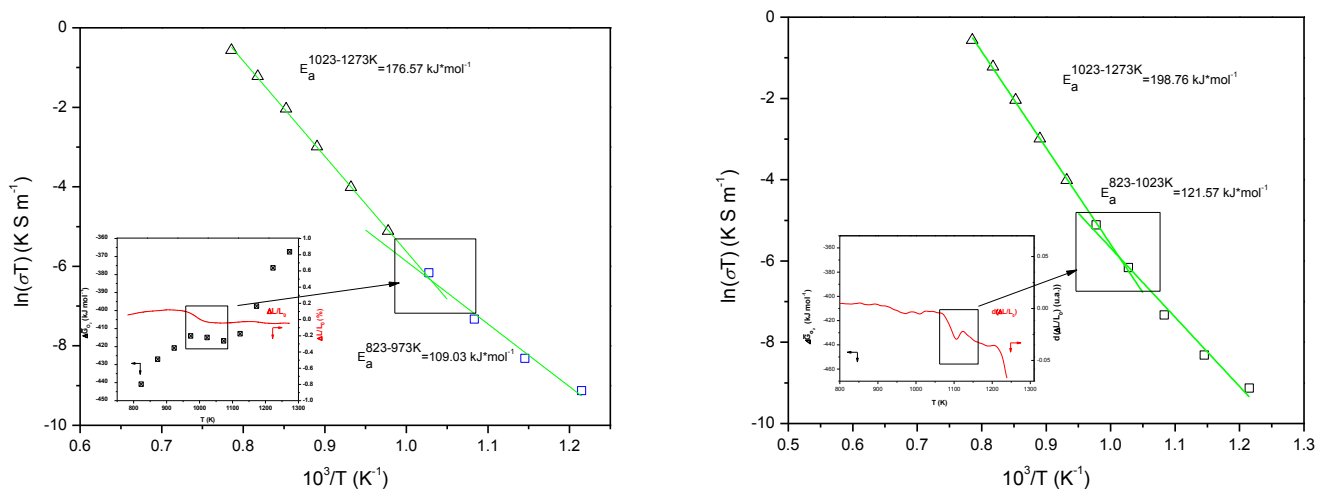


Figure 7. Temperature dependence of electrical conductivity of BST (left) and BST_Cu (right) in air; Inset: Relationship between thermodynamic, electrical and thermal expansion properties.

Evaluating the performance of gas sensors based on Ba_{0.75}Sr_{0.25}TiO₃ and (Ba_{0.75}Sr_{0.25})(Ti_{0.95}Cu_{0.05})O₃ metal oxide films

The BST and BST_Cu powders were deposited by screen printing on an alumina substrate with electrodes and platinum heater. After deposition, the substrates were left for one hour at room temperature to allow the films to fix, then dried at 353 K for 14 hours, followed by the heat treatment at 773 K for 45 min. The sensory performances of the BST and BST_Cu layers were investigated using the Gas Mixing Station (SMG) existing equipment in the INCDFM.

The BST_Cu sensor has a higher sensitivity towards H₂S than the BST sensor. The sensor signal for BST_Cu is 1 order of magnitude larger than BST. The different sensitivity of the two materials to H₂S can be explained by the differences between the properties of the materials. The specific surface area

of the BST_Cu powder is 2.2 times greater than that of BST, and the total BST_Cu pore volume is double then that of BST.

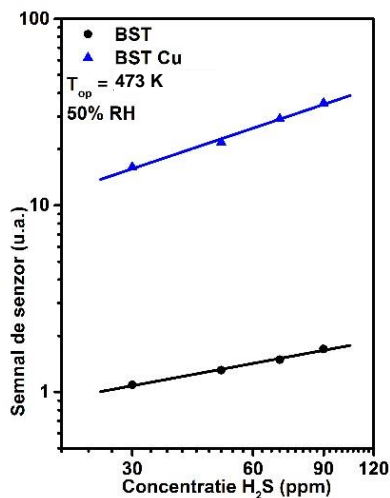


Figure 8. Sensor signal dependence for BST and BST_Cu sample exposed to H₂S in 50% relative humidity.

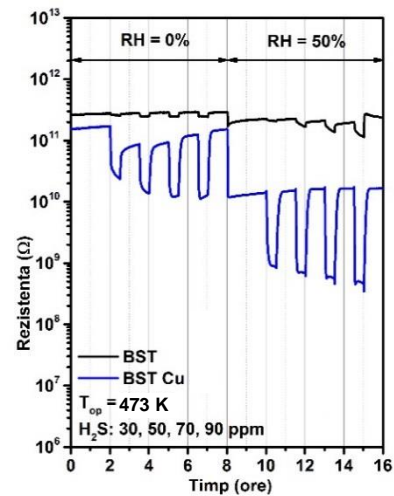


Figure 9. Variation of electrical resistance for BST and BST_Cu exposed to H₂S in different concentrations in dry air and humid air.

The presence of humidity leads to an increase in the ability of the sensitive film to bind a larger number of H₂S molecules. As a result, sensitivity under relative humidity conditions increases. This phenomenon probably occurs due to the influence of the high number of charged carriers on the combined effect of H₂S with pre-adsorbed oxygen and surface hydroxyl groups. It is noted that BST_Cu is more sensitive to H₂S than BST in both dry and humid conditions (Figure 9). For BST the resistance does not vary significantly, having a relatively low sensitivity to H₂S. Resistance to BST_Cu decreases of about one order of magnitude, a more pronounced decrease occurring in 50% relative humidity.

The study led to the following conclusions and original contributions:

- ▶ Ba_{0.75}Sr_{0.25}TiO₃ (BST) and (Ba_{0.75}Sr_{0.25})(Ti_{0.95}Cu_{0.05})O₃ (BST_Cu) nanocrystalline powders were synthesized by the hydrothermal method in aqueous medium. This is the first time when this method is used for Cu substitution in the barium strontium titanate lattice for the purpose of producing gas detection materials. The synthesis was the subject of a patent application (Patent Application OSIM A 00794 / 27.10.2014)
- ▶ Research on the microstructure, morphology and surface of the nanocrystalline powders Ba_{0.75}Sr_{0.25}TiO₃ and (Ba_{0.75}Sr_{0.25})(Ti_{0.95}Cu_{0.05})O₃ were performed. In order to identify the intermediate phases formed in the process of heating of the nanostructured powders, the structural and morphological analysis on the powders after the thermal treatment at 1073 K followed by cooling at room temperature has been performed. The results have highlighted the influence of dopants in positions A and B as well as the effect of thermal treatment on: the crystal size, the specific surface, the pore size, the lattice parameters, the microstructure and the powder morphology.
- ▶ For the first time, in this thesis a systematic study on thermochemical and thermodynamic stability of Ba_{0.75}Sr_{0.25}TiO₃ and (Ba_{0.75}Sr_{0.25})(Ti_{0.95}Cu_{0.05})O₃ nanocrystalline powders was

performed by combining several experimental methods in both dynamic and isothermal regimes (DSC/TG, drop calorimetry, EMF and solid state coulometric titration, TMA).

- ▶ The thermodynamic functions in the isothermal conditions (relative enthalpy, heat capacity, relative entropy and Gibbs free energy) of the hydrothermally obtained oxide powders $\text{Ba}_{0.75}\text{Sr}_{0.25}\text{TiO}_3$ and $(\text{Ba}_{0.75}\text{Sr}_{0.25})(\text{Ti}_{0.95}\text{Cu}_{0.05})\text{O}_3$ have been communicated for the first time within this thesis. The results confirm the increase of specific heat and entropy with the increase of nanocrystallinity, the minimum energy values indicating the range of stability of the nanostructured phases.
- ▶ The correlative effect of temperature and defect structure on the thermodynamic behavior of the samples was discussed based on the evolution of the thermodynamic quantities of the oxygen dissolution in the perovskite structure, also obtained for the first time in this thesis by using electromotive force measurements of solid electrolyte electrochemical cells (EMF) under equilibrium conditions. The influence of oxygen stoichiometry variations on thermodynamic properties was examined using solid state coulometric titration data coupled with EFM measurements.
- ▶ By determining the thermodynamic properties of strontium and copper doped barium titanate, information about variation of concentration and distribution of oxygen vacancies in the perovskite lattice has been obtained. The results evidenced the increase of the thermodynamic instability with the increase of the temperature and the role of the charge compensation mechanism in explaining the structural changes of the analyzed samples.
- ▶ Measurements of the relative linear variation of the $\text{Ba}_{0.75}\text{Sr}_{0.25}\text{TiO}_3$ and $(\text{Ba}_{0.75}\text{Sr}_{0.25})(\text{Ti}_{0.95}\text{Cu}_{0.05})\text{O}_3$ nanocrystalline samples were performed. Thermal expansion measurements performed in the temperature range 350-1273 K highlighted structural changes during heating and the correlations between thermodynamic stability, microstructure and thermal expansion were discussed.
- ▶ The resistivity and conductivity measurements were correlated with the thermodynamic properties and thermal expansion of the BST and BST_Cu samples. The conductivity activation energy in the 823-1023 K temperature range, as well as the partial molar enthalpy and entropy changes of the BST_Cu sample are higher than the conductivity activation energy values and the thermodynamic quantities of the BST sample, respectively.
- ▶ The BST and BST_Cu powders were used to prepare the films to be used in gas sensors. The conditions for the thermal treatment of the films were determined on the basis of the evolution of electrical properties, as well as considering the requirements for obtaining a crystalline film, but avoiding the growth of particles.
- ▶ The sensory performances of the BST and BST_Cu layers have been investigated. The experimental results demonstrated the superior performance of the BST_Cu sensitive film in the presence of H_2S in 50% relative humidity conditions and a working temperature of 473 K. The experimental work led to achieving of the prototype of a BST_Cu sensor.

ISI papers

1. C.F. Ruști, V. Badiliță, A.M. Sofronia, D. Taloi, E.M. Anghel, , F. Maxim, C. Hornoiu, C. Munteanu, R.M. Piticescu, S. Tănăsescu, Thermodynamic properties of the $Ba_{0.75}Sr_{0.25}TiO_3$ nanopowders obtained by hydrothermal synthesis, Journal of Alloys and Compounds 693, 2017, 1000–1010, IF=3.014.
2. C.E Simion, A. Sackmann, V.S. Teodorescu, C.F. Ruști, A. Stănoiu, Room temperature ammonia sensing with barium strontium titanate under humid air background, Sensors and Actuators B 220, 2015, 1241–1246, IF=4.097.
3. C.E. Simion, A. Stănoiu, V.Ș. Teodorescu, C.F. Ruști, R.M. Piticescu, E. Vasile, E. Vasile, I.A. Tudor, Ammonia sensing with 5 mol% lanthanum doped barium strontium titanate under humid air background, Revue Roumaine de Chimie 61(2), 2015, 105-111, IF=0.31.
4. C. Marinescu, A. Sofronia, C. Ruști, R. Piticescu, V. Badiliță, E. Vasile, R. Baies, S. Tănăsescu, DSC investigation of nanocrystalline TiO_2 powder, Journal of Thermal analysis and calorimetry 103, 2011, 49-57, IF=2.21.

Papers in Conference Proceedings

C.E. Simion, A. Sackmann, V.S. Teodorescu, C.F. Ruști, R.M. Piticescu, A. Stănoiu, Tuned sensitivity towards H_2S and NH_3 with cu doped barium strontium titanate materials, ELECTROCERAMICS XIV CONFERENCE Book Series: AIP Conference Proceedings, 1627, **2014**, 92-97.

Paper under review

A. Stănoiu , R. M. Piticescu , C. E. Simion , C. F. Ruști-Ciobota , O. G. Florea , V. S. Teodorescu , P. Osiceanu , A. Sobetkii , V. Bădiliță, H_2S selective sensitivity of Cu doped $BaSrTiO_3$ under operando conditions and the associated sensing mechanism, trimisa la Sensors & Actuators, B: Chemical

Patents

1. OSIM No. 128625/2014 Title: “Portland cement with fly ash added with ZnO nanoparticles” Inventors: Mohanu Ileana, Paceagiu Jenica, Moantă Adriana, Roxana Mioara Piticescu, Ruști Cristina Florentina.
2. OSIM No. 129568/2017 Title: “In-situ hydrothermal-electrochemical process for the preparation of nanostructured substrates of cobalt-doped titanium dioxide” Inventors: Piticescu Radu Robert, Ruști Cristina Florentina, Piticescu Roxana Mioara, Popescu Laura Mădalina